Ocean Modelling 26 (2009) 104–113

Contents lists available at ScienceDirect

Ocean Modelling

journal homepage: www.elsevier.com/locate/ocemod

The effect of dynamic–thermodynamic icebergs on the Southern Ocean climate in a three-dimensional model

Jochem I. Jongma [a,*], Emmanuelle Driesschaert [b], Thierry Fichefet [b], Hugues Goosse [b], Hans Renssen [a]

[a] Paleoclimatology and Geomorphology, Faculty of Earth and Life Sciences, Vrije Universiteit Amsterdam, Boelelaan 1085, NL-1081HV Amsterdam, The Netherlands
[b] Institut d'Astronomie et de Géophysique Georges Le maître, Université Catholique de Louvain, Louvain-la-Neuve, Belgium

ARTICLE INFO

Article history:
Received 25 December 2007
Received in revised form 11 September 2008
Accepted 18 September 2008
Available online 10 October 2008

Keywords:
Climate
Model
Icebergs
Meltwater
Southern Ocean
Convection
Sea-ice

ABSTRACT

Melting icebergs are a mobile source of fresh water as well as a sink of latent heat. In most global climate models, the spatio-temporal redistribution of fresh water and latent heat fluxes related to icebergs is parameterized by an instantaneous more or less arbitrary flux distribution over some parts of the oceans. It is uncertain if such a parameterization provides a realistic representation of the role of icebergs in the coupled climate system. However, icebergs could have a significant climate role, in particular during past abrupt climate change events which have been associated with armada's of icebergs. We therefore present the interactive coupling of a global climate model to a dynamic thermodynamic iceberg model, leading to a more plausible spatio-temporal redistribution of fresh water and heat fluxes. We show first that our model is able to reproduce a reasonable iceberg distribution in both hemispheres when compared to recent data. Second, in a series of sensitivity experiments we explore cooling and freshening effects of dynamical icebergs on the upper Southern Ocean and we compare these dynamic iceberg results to the effects of an equivalent parameterized iceberg flux.

In our model without interactive icebergs, the parameterized fluxes are distributed homogeneously South of 55°S, whereas dynamic icebergs are found to be concentrated closer to shore except for a plume of icebergs floating North–East from the tip of the Antarctic Peninsula. Compared to homogeneous fluxes, the dynamic icebergs lead to a 10% greater net production of Antarctic bottom water (AABW). This increased bottom water production involves open ocean convection, which is enhanced by a less efficient stratification of the ocean when comparing to a homogeneous flux distribution.

Icebergs facilitate the formation of sea-ice. In the sensitivity experiments, both the fresh water and the cooling flux lead to a significant increase in sea-ice area of 12% and 6%, respectively, directly affecting the highly coupled and interactive air/sea/ice system. The consequences are most pronounced along the sea-ice edge, where this sea-ice facilitation has the greatest potential to affect ocean stratification, for example by heat insulation and wind shielding, which further amplifies the cooling and freshening of the surface waters.

1. Introduction

Many climate models predict an abrupt climate change following a (partial) collapse of the thermohaline circulation under influence of freshwater perturbations (Petoukhov et al., 2005; Rahmstorf et al., 2005; Stouffer et al., 2006). In the last glacial climate, one important source of such freshwater perturbations were large armadas of icebergs known as Heinrich events (Heinrich, 1988; Bond et al., 1992). In the present climate, iceberg fluxes are much smaller, but their effect on climate might still be significant and correlations have been found between iceberg rafting and Holocene climate variability (Bond et al., 2001). However, as presently none of the global coupled three-dimensional climate models incorporates interactive dynamic icebergs, it has not yet been possible to study the interaction between icebergs and ocean circulation in detail. We therefore present a two-way (interactive) coupling of a global climate model to a dynamic thermodynamic iceberg model and investigate its performance for the modern pre-industrial climate.

Melting icebergs can have two direct effects on deep water formation. First, the melting generates a fresh water flux, which lowers water density. On the other hand icebergs cool their surroundings when they melt, increasing water density. These effects can be expected to alter the vertical density profile, affecting the character of the pycnocline and the stability of the upper water column (e.g. Martinson, 1990a,b). Consequently, icebergs are a mobile mediator of deep water formation.

* Corresponding author. Tel.: +31 205989807.
E-mail address: jochem.jongma@falw.vu.nl (J.I. Jongma).

1463-5003/$ - see front matter © 2008 Elsevier Ltd. All rights reserved.
doi:10.1016/j.ocemod.2008.09.007

Furthermore, a freshening and cooling of surface waters might be expected to facilitate the formation of sea-ice, influencing the climate through several feedbacks. An extended sea-ice cover leads to atmospheric cooling through the positive ice-albedo (Covey et al., 1991; Manabe et al., 1992) and heat-insulation feedbacks (e.g. Martinson, 1990a,b). Because of the insulation, and also by shielding the ocean from strong wind mixing, sea-ice formation can lead to increased stratification of the upper water column, inhibiting convection. Negative feedbacks, which enhance salinity and promote deep water formation, include the brine rejection associated with sea-ice formation, and the interception of precipitation by the sea-ice (e.g. Martinson, 1990b; Gordon 1991).

We have coupled a dynamic iceberg module to ECBilt-CLIO, a global atmosphere–ocean–sea-ice model of intermediate complexity (Opsteegh et al., 1998; Goosse and Fichefet, 1999). The dynamics and thermodynamics of our iceberg-module are based on the iceberg-drift model introduced by Smith (Smith, 1993) and further developed by Bigg et al. (1996, 1997). This model predicts the path of a melting iceberg. In previous studies, the resulting iceberg dynamics have been investigated by prescribing observed modern average climate fields in the Arctic (Bigg et al., 1996) as well as the Antarctic (Gladstone et al., 2001) region. For the paleoclimate, iceberg trajectories have been simulated under different LGM states by prescribing climatic output from a climate modelling under fixed wind conditions (Bigg et al. 1998). Furthermore, the dynamics of icebergs released from a Scandinavian ice sheet under glacial conditions have been investigated (Death et al., 2006), and modelled North Atlantic iceberg trajectories have been used to investigate the plausibility of alternative LGM ocean circulation states (Watkins et al., 2007). These studies with prescribed boundary conditions have allowed for a detailed high-resolution investigation of iceberg dynamics and melting fluxes, but have not yet taken into the account the effects that the melting icebergs might have on the climate.

To investigate the complex effects that icebergs might have on climate, we have coupled the iceberg module interactively with an intermediate complexity climate model, by adding the fresh water and latent heat fluxes associated with the iceberg melt to the surface ocean layer of the local grid cell. Using a series of sensitivity experiments, we have delineated the three main effects of icebergs (distribution, freshening and cooling) on the modelled dynamics of the Southern Ocean. We focus on the Antarctic surface ocean response on a multi-decadal time-scale because iceberg fluxes are highest in the South and because we aim to avoid the three-dimensionally complex North Atlantic, which can for example exhibit memory effects on a multi-centennial time-scale (Jongma et al., 2007), from interfering with our interpretation of the sensitivity experiments. The performance of our ocean model in the Southern Ocean has been analysed in detail in previous publications (Goosse and Fichefet, 2001; Beckmann and Goosse 2003). It should be noted that it is not our primary intention here to analyse how the introduction of an interactive iceberg model could improve the quality of model results. Our goal is rather to analyse the feedbacks that are associated with icebergs.

First we will show that this coupled iceberg model gives acceptable predictions of iceberg tracks in the modern (i.e. pre-industrial) climate. Then we will study the averaged impact of dynamic–thermodynamic icebergs on the Southern Ocean. The spatial effects of the icebergs' fresh water fluxes and latent heat fluxes on the surface ocean, sea-ice formation and Antarctic convection are presented, after which the net effects are discussed.

2. Methods

2.1. ECBilt-CLIO

ECBilt-CLIO (version 3) is a three-dimensional global coupled atmosphere–ocean–sea-ice model. Although ECBilt-CLIO has a reasonably elaborate ocean, it is comparatively fast thanks to its atmosphere, which combines a relatively coarse resolution and simplified radiation scheme with the quasi-geostrophic approximation that allows for a larger time-step. Therefore, ECBilt-CLIO is also known as an Earth system model of intermediate complexity (Claussen et al., 2002).

The oceanic module CLIO is a $3^\circ \times 3^\circ$-resolution, 20-level, primitive equation, free-surface ocean general circulation model (Deleersnijder and Campin, 1995; Campin and Goosse, 1999) coupled to a thermodynamic–dynamic sea-ice model (Goosse and Fichefet, 1999). It includes a detailed formulation of boundary layer mixing based on Mellor and Yamada's (1982) level-2.5 turbulence closure scheme (Goosse and Fichefet, 1999), a parameterization of density-driven down-slope flows (Campin and Goosse 1999), and a discretised bathymetry. The ocean has a 1-day time-step, which is also used for the iceberg model. The atmospheric module ECBilt is a T21, three level quasi-geostrophic atmospheric model with a 4-h time step (Opsteegh et al., 1998). Its purpose is to provide the ocean with appropriate atmospheric feedbacks. A simple moisture-budget water-bucket model is used for the land area, with all run-off instantly distributed over a designated ocean area, corresponding to associated river catchments. When temperatures are below freezing point, precipitation is presumed to be in the form of snow. For a more extensive description of ECBilt-CLIO see: http://www.knmi.nl/onderzk/CKO/ecbiltdescription.html.

In ECBilt-CLIO, like in many climate-models, the global precipitation and heat budget is kept closed by redistributing all snow above a certain threshold over a designated ocean area, which is a way to parameterize iceberg-calving. For example, Antarctic icebergs are parameterized by removing all snow-accumulations above 10 m and distributing the amount of fresh water and melting-heat this snow represents evenly over the Southern Ocean south of 55°S, while in the Arctic the excess snow is redistributed through the corresponding river run-off scheme.

In all experiments described below this redistribution of excess snow is disabled. Instead, iceberg fluxes are prescribed based on observations as opposed to modelled precipitation. To close the mass balance, the prescribed fresh water flux is globally compensated. The resulting correction for the global surface ocean is of the order of 3×10^{-4} m of water per year, which should be kept in mind when interpreting the results.

2.2. Iceberg model

2.2.1. Iceberg dynamics

The dynamics and thermodynamics of our iceberg-module are based on the iceberg-drift model introduced by Smith (Smith and Banke, 1983; Loset, 1993; Smith, 1993) and further developed by Bigg et al. (1996, 1997). Empirical parameters include drag coefficients, reflecting the exchange of momentum between the iceberg and the ocean, the atmosphere and the sea-ice, and melting coefficients, which determine the relative importance of basal melt, side melt and wave erosion and ultimately dictate the melting speed of the icebergs. In this study we have adopted all parameter choices of Bigg et al. (Bigg et al. 1996, 1997; Gladstone et al. 2001). Accordingly, our analysis of the iceberg distribution will evolve around a comparison with the iceberg limits suggested by Gladstone et al. (2001) (see Fig. 1).

The iceberg model predicts the path of an iceberg subject to Coriolis force ($Mf\vec{k}\times\vec{k}$), air drag ($\vec{F}_a$), water drag ($\vec{F}_w$), sea-ice drag ($\vec{F}_s$), horizontal pressure gradient force ($\vec{F}_p$) and wave radiation force ($\vec{F}_r$).

$$M\frac{d\vec{V}_i}{dt} = -Mf\vec{k}\times\vec{V}_i + \vec{F}_a + \vec{F}_w + \vec{F}_s + \vec{F}_p + \vec{F}_r \quad (1)$$

where $\vec{V}_i$ is the velocity (m/s) of the iceberg with mass M (kg). The general drag relationship is (Smith, 1993):

$$\vec{F}_x = \frac{1}{2}\rho_x C_x A_x \left|\vec{V}_x - \vec{V}_i\right|\left(\vec{V}_x - \vec{V}_i\right) \quad (2)$$

where x refers to air (a), water (w) or sea-ice (s), ρ_x is the density (kg/m^3) of the appropriate medium, C_x is the drag coefficient ($C_a = 1.3$, $C_w = 0.9$ (Smith, 1993) and $C_s = C_w$ (Bigg et al., 1997; Gladstone et al., 2001) and A_x is the cross-sectional area of the iceberg perpendicular to the stressing medium, which has velocity $\vec{V}_x$ (m/s), where the iceberg is assumed to be travelling with its long axis parallel to the surrounding water and sea-ice flow and at an angle of 45° to the wind flow, in accordance with Ekman theory (Bigg et al., 1997). Thus $A_w = A_s = 1$ and $A_a = |1.5\sin(45)| + |\cos(45)| \approx 1.77$. In practice, many icebergs undergo an inertial rotation so this approach can only be approximate. It has given good descriptions of the general behaviour of icebergs but cannot be expected to work well for individual bergs (G.R. Bigg, personal communication). Water stress acting along the lower surface of the iceberg and atmospheric wind stress acting along the top surface are deemed negligible, since the corresponding drag coefficients are relatively small (0.0055 instead of 0.9 for water and 0.0012 instead of 1.3 for air (G.R. Bigg, personal communication). Note that the drag coefficients of an individual iceberg would depend on its shape. We use mean estimates because of the smoothness of the forcing fields and because our goal is to simulate general iceberg distribution rather then exact trajectories of individual icebergs. The wave radiation force is (Smith, 1993):

$$\vec{F}_r = \frac{1}{4}\rho_w g a^2 L \frac{\vec{V}_a}{|\vec{V}_a|} \quad (3)$$

where L is the length of the iceberg perpendicular to incident waves with amplitude a which are assumed to have the same direction as wind velocity $\vec{V}_a$ (g is the gravitational constant).

In this dynamical model, added mass due to entrained melt water is neglected. A difference with iceberg dynamics implemented by Bigg et al. (1997) is the treatment of the horizontal pressure gradient force exerted on the water volume that the iceberg displaces ($\vec{F}_p$). Since the icebergs are forced with a free-surface ocean, we don't need to resort to a principal factor approximation of this pressure, but can take it directly from the ocean model's dynamic variable at the iceberg's location (Deleersnijder and Campin, 1995).

The strength of the climate models forcing fields at the iceberg's location is interpolated linearly from the four surrounding grid corners. There is no direct interaction, such as collisions, between icebergs. Keel shape or other turbulence related effects are not accounted for.

2.2.2. Iceberg thermodynamics

The mass and the shape of an iceberg constantly change due to melting, which means an iceberg's thermodynamics must be accounted for in any long term simulation of its trajectory. Following an empirical approach (Bigg et al., 1997), the iceberg melt is simplified to basal melt, lateral melt and wave erosion. The parameterization for basal turbulent melting rate (Weeks and Campbell, 1973)

$$M_{basal} = 0.58\left|\vec{V}_W - \vec{V}_i\right|^{0.8}\frac{T_s - T_i}{L^{0.2}} \quad (4)$$

involves a difference between iceberg ($T_i = -4$ °C) and sea surface temperature (T_s). An empirical relationship (Eltahan et al., 1983)

$$M_{lateral} = 7.62\times10^{-3}T_W + 1.29\times10^{-3}T_W^2 \quad (5)$$

describes the lateral melt due to buoyant convection along the sides of the iceberg as a function of water temperature T_w (°C) of the corresponding ocean layer in the local grid cell. Wave erosion (Bigg et al., 1997)

$$M_{waves} = 0.5\ S_S \quad (6)$$

is taken as a function of sea state S_S

$$S_S = -5 + \sqrt{32 + 2|\vec{V}_a|} \quad (7)$$

which is based on the definition of the Beaufort scale, and involves the magnitude of air velocity $\vec{V}_a$ (km/h).

Due to the large heat capacity of water, iceberg deterioration by atmospheric and radiation effects is marginal (Loset, 1993) and considered to be negligible. The icebergs are assumed to remain tabular and maintain a constant length to width ratio of 1:1.5, which is in reasonable agreement with observations (see Bigg et al., 1997). They are allowed to roll over when the ratio between iceberg length L and height H exceeds a criterion of stability (Bigg et al., 1997)

$$\frac{L}{H} = \sqrt{0.92 + \frac{58.32}{H}} \quad (8)$$

but break-up of icebergs is not modelled. When hitting the coast, the icebergs are weakly repelled using a velocity of 0.003 m/s in a direction orthogonal to the land–sea boundary. Following Gladstone et al. (2001), the icebergs become grounded when their keel exceeds water depth, remaining stationary until they have melted sufficiently.

To achieve climatic coupling, the fresh water and latent heat fluxes associated with the iceberg melt are added to the surface ocean layer of the local grid cell, which in turn affects the atmosphere. Possible direct feedbacks from the icebergs to the atmosphere, are relatively small (e.g. Loset, 1993) and are not accounted for.

2.2.3. Iceberg generation

Involving topographic details of the sub-glacial rock-bed, iceberg calving remains one of the most poorly understood ice sheet mechanisms. However, the accurateness of the iceberg budget is considered to be of minor importance for our results, since we take a sensitivity approach, focusing our analysis on a comparison between experiments with identical flux-budgets.

Icebergs of various size classes are produced at appropriate calving sites, with a fixed yearly production rate. The calving sites are based on observations of glacier and ice sheet calving, complimented with ad hoc iceberg sources where observations are scarce. The total yearly budget of Antarctic iceberg calving of 1.98×10^{14} kg/yr is based on a mass balance estimate (Zotikov et al., 1974) and can be considered to be in the high end of calving estimates. The size-distribution of the icebergs follows a log normal distribution (Wadhams, 1988; Bigg et al., 1996) with no seasonal dependence. There are 14 size classes, with 76% in size classes 3–6. Effectively there is a sharp decline in icebergs larger then 1 km and a relatively large number of icebergs measure less then 500 m in length (Weeks and Mellor, 1978; Wadhams, 1988; Dowdeswell et al., 1992). A detailed overview of the iceberg pro-

duction, including coordinates of the production sites, yearly budget and maximum iceberg height, can be found online on pages 30–33 of (Driesschaert, 2001) (link is available at: http://www.astr.ucl.ac.be/index.php?page=LOVECLIM%40Description).

2.3. Experimental set up

Since this is the first time that the coupled model is described we will start with a distribution map of iceberg fluxes in both hemispheres (see Section 3.1). The uncertainty in the modelled iceberg distribution as well as in modern day observations can be expected to be quite large. To evaluate the effect that dynamic icebergs have on climate, we therefore adopt a sensitivity approach (Sections 3.2 and 3.3) where we base our analysis on a comparison between different model set-ups, with a constant yearly budget of iceberg production. Focusing on the Southern Ocean, this sensitivity study explores the following effects of the melting icebergs: (i) freshening effect (ii) cooling effect and (iii) dynamic distribution effect. An overview of the sensitivity experiments is given in Table 1. For each experiment listed, (X) marks whether the interactive iceberg's fresh water flux (FWF) and/or latent heat flux (LHF) is activated.

As equilibrium baseline, the model with fully active icebergs (i.e. including cooling and freshening effect, hereafter ICB) was run 900 years under pre-industrial (1750 AD) boundary conditions. For each of the sensitivity experiments, 13 ensemble-member runs were performed, each started with initial conditions derived from this ICB equilibrium at 100-year intervals. We have chosen this experimental design because we are mostly interested in the direct effect of icebergs on decadal timescales, and specifically in the interaction with sea-ice in the Southern Hemisphere. On a longer time-scale, feedbacks from the deep ocean and the Northern Hemisphere could have gotten involved (e.g. Stocker et al., 1992; Seidov et al., 2001; Stouffer et al., 2007), which would have hampered the interpretation of the direct response in the Southern Ocean. In our 100-year experiments, the surface ocean is reasonably stabilized after about 50 years (for example, see Fig. 4). Accordingly, for our analysis of the mean response of the Southern Ocean on a multi-decadal time-scale, the first 50 years of each 100-year experiment are discarded to reduce the error associated with decadal scale response delay.

To separate the cooling effect from the freshening effect, two experiments were run with partly inactive icebergs (hereafter COOL and FRESH). These two sensitivity experiments are compared with an experiment with inactive icebergs (hereafter DUMMY). In short, the FRESH minus DUMMY anomaly provides an estimate of the freshening effect, whereas the COOL minus DUMMY anomaly is used to quantify the cooling effect (Table 2).

The interactive icebergs (ICB) will result in a spatial and temporal redistribution of the fluxes. To investigate this distribution effect (Table 2), we compare the results of ICB with a control experiment (hereafter CTL) that was conducted with a classical distribution (see Section 2.1) of the melt water and heat fluxes that are associated with the prescribed Southern Hemisphere iceberg production. The CTL experiment has homogeneously distributed fluxes as opposed to interactive icebergs, but the same prescribed total Southern Hemisphere iceberg-flux budget as the other experiments. The DUMMY experiment has zero fluxes.

Table 1
Overview of activated (X) fluxes in the sensitivity experiments discussed in this study. See Section 2.3 for details.

Flux Exp.	Iceberg FWF	Iceberg LHF	Homog. fluxes
ICB	X	X	–
COOL	–	X	–
FRESH	X	–	–
CTL	–	–	X
DUMMY	–	–	–

Table 2
Interpretation of anomalies mapped in Fig. 3. See Section 2.3 for details (see also Tables 1 and 3).

Anomaly	Interpretation	Figure
FRESH–DUMMY	Freshening effect	Fig. 3B
COOL–DUMMY	Cooling effect	Fig. 3C
ICB–DUMMY	FRESH and COOL combined	Fig. 3D
ICB–CTL	Distribution effect	Fig. 3E

3. Results and discussion

3.1. Distribution of the interactive icebergs

The simulated distribution of the interactive icebergs compares reasonably well with observations. The iceberg distribution is visualized by plotting the melting fluxes in the North Atlantic (Fig. 1) and in the Southern Ocean (Fig. 2). Due to the sporadic nature of iceberg observations, validation of the iceberg distribution is more qualitative than quantitative.

In the North Atlantic, iceberg observations mostly consist of historic logs of hazards along the main shipping routes, from which extreme sightings can be reconstructed (dots in Fig. 1). Near Newfoundland, long term observations by the international ice patrol have allowed for a well-documented modern iceberg limit in that area (solid line in Fig. 1).

For Antarctica, a rough estimate of the modern iceberg limit (dashed line in Fig. 2) comes from a Russian exploration in 1964.The solid line gives the maximum Northern extent of iceberg sightings according to data combined from numerous sources by Robe (1980). However, incidental icebergs have been observed far beyond this limit, for example the northern-most recorded

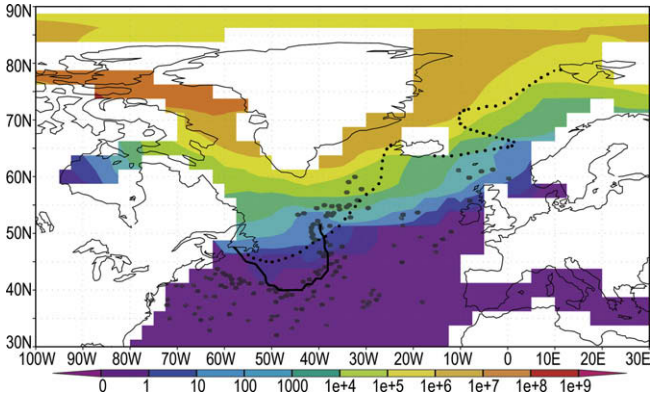

Fig. 1. Distribution of simulated iceberg melt in the North Atlantic Ocean. The average volume flux of fresh melt water per day (m^3/day) provides a combined insight in the distribution of the dynamic icebergs and their melting speed. Note logarithmic scale. Dotted line represents iceberg limit simulated by Gladstone et al. (2001). Dots are historic iceberg and growler sightings from ships logs going back ca. 150 years (adapted from Bond et al., 1999). The solid line is the May 30 extreme based on sightings by the International Ice Patrol between 1945 and 1974 near Newfoundland (http://www.uscg.mil/lantarea/iip/General/45_74BergClimo_Images/May30_1945-). The iceberg melting flux distributions in Figs. 1 and 2 are based on a 100-year average of ensemble member 3 of the ICB run.

sighting in the Southern Hemisphere was at 26°30′S, off Brazil, while another low-latitude sighting was in 1828, at 35°50′S, 18°05′E, where clusters of icebergs of 30 m freeboard were observed. (Wadhams, 2007).

Compared to the parameterized (CTL) homogeneous flux distribution around Antarctica, the fluxes from the dynamic icebergs are more concentrated near shore (Fig. 2). Please note that the volume flux from the melting icebergs is given on a logarithmic scale. This means that e.g. the flux in the yellow area is 100.000 times greater than the dark blue flux. Of course, the latent heat flux associated with the iceberg-melt mimics this distribution.

At first glance Fig. 2 might appear to indicate that the icebergs in our study get much further than the modelled iceberg limit suggested by Gladstone et al. (2001). However, the bulk (yellow/green limit) of our distribution agrees reasonably well with the iceberg limit modelled by Gladstone et al. (2001). A larger variance can be expected in our results due to a different experimental set-up, since Gladstone et al. (2001) forced the iceberg movement by prescribing fixed wind fields and ocean currents, whereas in our set-up the icebergs interact with a climate model that simulates variability in the ocean and atmosphere on various timescales. Furthermore, the total number of simulated ICB icebergs in our study is orders of magnitude higher. The coarser resolution of our model might also be responsible for some of the differences.

Interestingly, our results confirm the 'tongue' of icebergs coming off the Antarctic Peninsula, which might be interpreted as an illustration of the limited resolution of the observed limit, where this shape is absent. It seems our icebergs stay closer to shore in the Pacific sector of Antarctic, near the Ross Sea, which might be partly due to the limited resolution of the ocean model. In reality, and in the Gladstone et al. (2001) results that were obtained with higher resolution ocean forcing, icebergs from the Ross Ice Shelf, tend to get entrained in a jet-like current that flows out from the coast in the western Ross Sea area. There are similar, although less effective, offshore currents in the Kerguelen area and the eastern end of the Weddell Sea which a 3×3 degree model might also struggle to resolve.

In the North Atlantic, apparently the bulk of our icebergs drift slightly less to the South. It is not unlikely that a high-resolution ocean model might capture iceberg drift in the southward flowing coastal current along North Eastern America more effectively. The icebergs also drift further to the East than the modelled limit suggested by Bigg et al. (1996) (dotted line in Fig. 1). However, the uncertainties both in the observations and in the models could very well be larger than this discrepancy, especially when we recall that we can expect a larger variance in our dynamic iceberg trajectories due to the different experimental set-up. This is illustrated by the fact that there are numerous iceberg observations beyond the Gladstone et al. (2001) limit, many of which are quite consistent with our results (dots in Fig 1). The coarser resolution of our model might also be responsible for some of the differences.

Recalling that we prescribed pre-industrial as opposed to present day boundary conditions, we tentatively conclude that the distribution of interactive icebergs is not inconsistent with other iceberg modelling studies nor with observations. More quantitative observations might allow for further constraints on the iceberg dynamics and/or thermodynamics in the future.

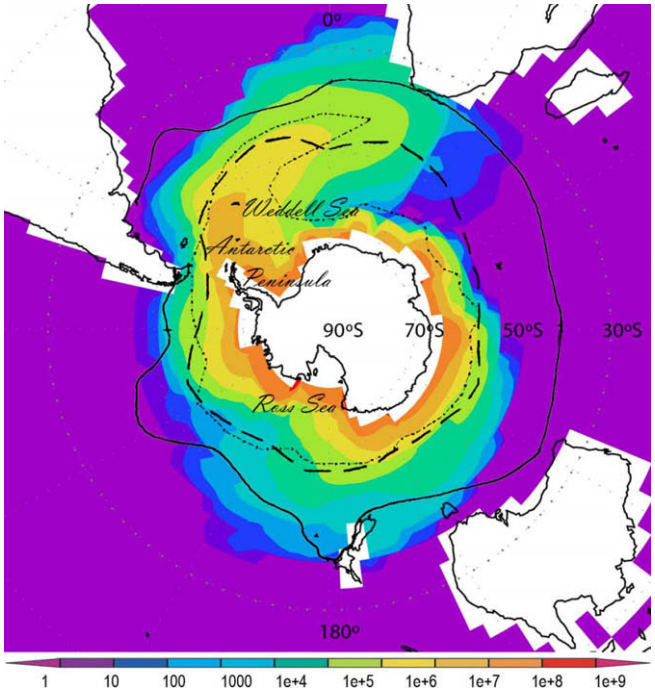

Fig. 2. Distribution of simulated iceberg melt in the Southern Ocean. The average volume flux of fresh melt water per day (m^3/day) provides a combined insight in the distribution of the dynamic icebergs and their melting speed. Note logarithmic scale. Dotted line is the iceberg limit in the Southern Ocean as simulated by Gladstone et al. (2001). Dashed line is an estimate from Russian exploration in 1964 (adapted from Gladstone et al., 2001). The solid line is an estimate of maximum iceberg extent based on a large collection of observational data (adapted from Robe, 1980).

3.2. Sensitivity study in the Southern Ocean: salinity, temperature, sea-ice and convection anomalies

In a series of sensitivity experiments, we explored the effect of the icebergs on the Southern Ocean. In Fig. 3A, sea surface salinity (SSS) and temperature (SST) as well as sea-ice fraction (SICE) and convective layer depth (CLD) are given for the ICB experiment. These maps of the Southern Hemisphere are given as reference for the anomalies mapped in Fig. 3B–E (see also Table 2).

The SSS is most affected by the FRESH icebergs melt water fluxes (Fig. 3B–I). Where the melting fluxes are strongest (see Fig. 2), a salinity reduction in the order of 0.3 psu can be observed. While the Weddell Sea and, to a lesser extent, the outer Ross Sea show an increase in salinity, there is a band of ~0.1 psu freshening around 60°S. Interestingly, a similar freshening can be observed for the COOL icebergs (Fig. 3C–I) near the Antarctic Peninsula (between 120°W and 30°E). The combined cooling and freshening effect (Fig. 3D–I) looks like a simple sum of these two effects. The distribution effect (Fig. 3E–I) is more complex: a freshening that mimics the FRESH effect in the Indian and Pacific sector is complemented by a saltier Atlantic section.

A very similar picture emerges for the SST. While the COOL icebergs (Fig. 3C-II) induce a significant cooling (especially in the Pacific and Atlantic sectors between 150°W and 60°E), the FRESH icebergs (Fig. 3B-II) have the strongest impact, especially between 50°S and 60°S. Although this cooling seems absent in the eastern part of the Indian sector, the combined effect (Fig. 3D-II) is a 0.5–2 °C cooling between 50°S and 60°S all around Antarctica, which is only interrupted off the tip of the Antarctic Peninsula and South of New-Zealand, where a warm anomaly is present in the FRESH, respectively, COOL experiment. Presumably these warm anomalies are related to small (grid-size scale) changes in the sea-ice cover and/or the ACC path. The absence of strong cooling south of ~68°S is most likely due to the year round 100% sea-ice cover in that area (Fig. 3A-III), which maintains the SST close to melting temperature. The dynamically distributed icebergs result in a cooler Pacific but warmer Atlantic and Indian sector than the homogeneous flux distribution (ICB–CTL; Fig. 3E-II), although there is some

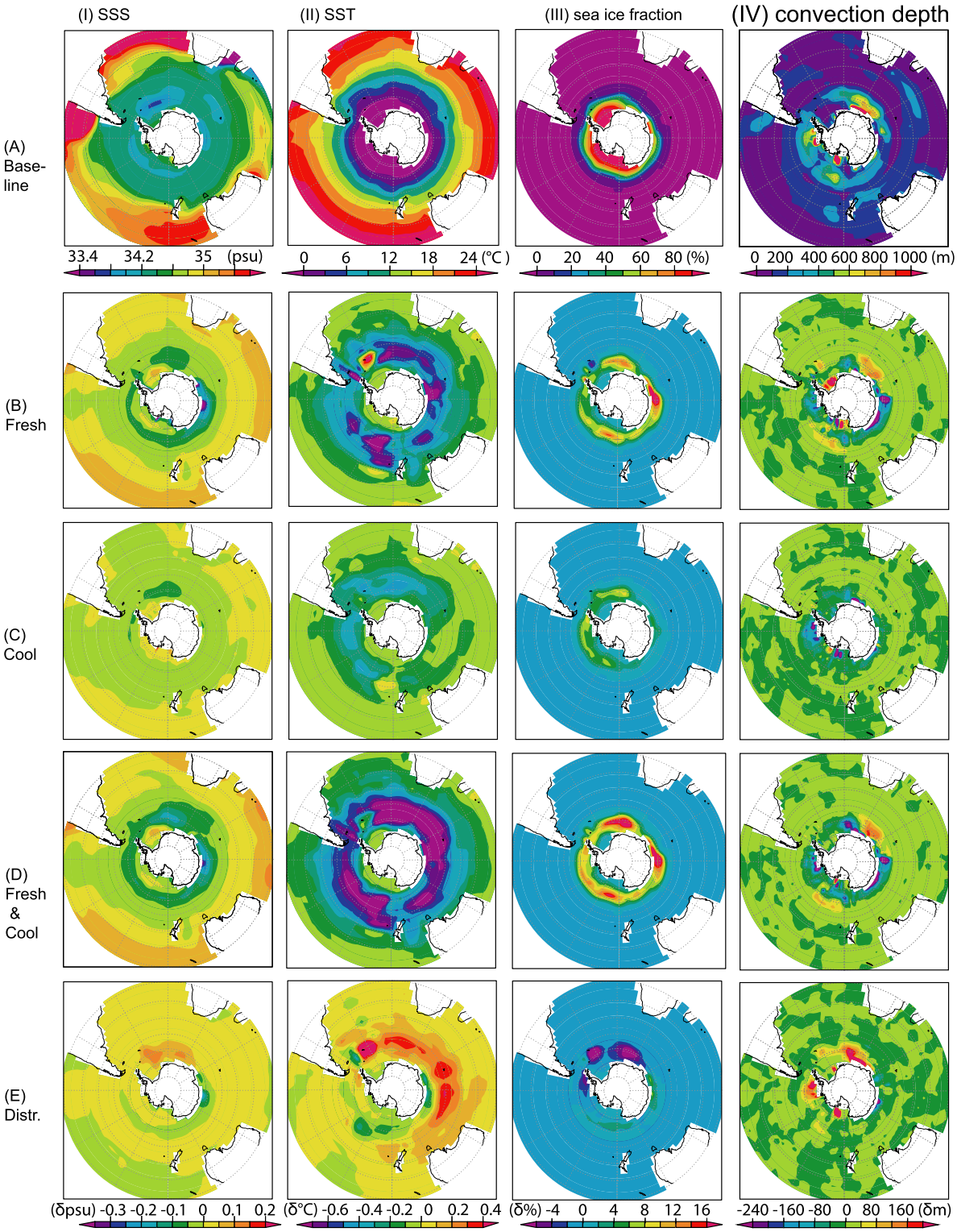

Fig. 3. (I-A to IV-E) Anomalies in average Southern Hemisphere (from left to right) I: sea surface salinity (SSS), II: sea surface temperature (SST), III: sea-ice fraction and IV: convection layer depth. Top to bottom: (A) ICB ensemble average; (B) freshening effect (FRESH–DUMMY); (C) cooling effect (COOL–DUMMY); (D) combined effect (ICB–DUMMY); and (E) distribution effect (ICB–CTL). These are 13-member ensemble averages over the second 50 yearly averages of each member. Hence these patterns are robust but smoothed, meaning the magnitude of the anomalies might be underestimated. To provide a more informative map of the by nature episodical CLD, (ensemble averages of) the maxima (for each gridcell the maximum CLD in 50 * 12 months) were used. However, the scale was adjusted to enhance detail and comparability. Actual scale-ranges were (in meters): (A-IV) 0–2700; (B-IV) −1000 to 200; (C-IV) −700 to 100; (D-IV) −600 to 800; (EIV) −400 to 1000. See also Table 2 and Table 3.

near shore cooling in the eastern Indian section where iceberg melt is high.

The anomalous sea-ice fraction displays strong spatial similarity with the SSS and SST. The FRESH (Fig. 3B-III) icebergs cause a strong increase around 60°S, that peaks near the shore of the Indian sector, and combines (Fig. 3D-III) with a COOL effect (Fig. 3C-III) that is strongest in the Pacific and Atlantic sector. A sea-ice decrease in the Atlantic sector is complemented by increase

elsewhere when comparing the icebergs with homogeneous fluxes (Fig. 3E-III).

The anomalies in the convective layer depth look more complex. As might be expected, convection anomalies are greatest where convection is strongest (Fig. 3A-IV). Most of the positive anomalies in the FRESH and COOL experiments (Fig. 3B-IV–D-IV) appear alongside negative anomalies in dipole-patterns, which could indicate spatial shifts in the major convection sites (see also Fig. 3A-IV). The inhibitive (negative) FRESH effects (Fig. 3B-IV) are strongest in the eastern Indian Ocean sector, but also occur elsewhere along the 60°S as well as in the Pacific sector. As might be expected, the COOL icebergs (Fig. 3C-IV) lead to an increased convection depth, and greater overturning (Antarctic bottom water production, represented by the maximum of the global stream function in the Southern Ocean, is 4.5% stronger on average, see Table 3). Again the COOL and FRESH effects more or less add up for the fully active icebergs (ICB minus DUMMY, Fig. 3D-IV). Comparing these combined iceberg effects with the classical parameterisation results (ICB minus CTL; Fig. 3E-IV), the interactive dynamical icebergs lead to a greater convection depth in the Atlantic and eastern Pacific sectors and weaker convection east of 60°E. The increase in the Eastern Weddell Sea occurs in an area where iceberg flux is relatively weak. It results in stronger mixing with deep water in this area and finally contributes significantly to the higher salinity, higher SST and lower ice concentration in this region in ICB compared to the CTL experiment with homogeneous flux distribution.

3.3. Impact of icebergs on sea-ice formation and stratification

The spatial similarities between the SSS, SST and sea-ice anomalies demonstrate that both the freshening and the cooling effect facilitate the formation of sea-ice. This is confirmed by the time-series of the total sea-ice area in the Southern Hemisphere (Fig. 4), showing that both the FRESH icebergs (red curve) and the COOL icebergs (yellow) lead to considerably more sea-ice compared to the DUMMY experiment (purple).

We can quantify this sea-ice facilitation by taking an average over the second 50 years of these 100-year time-series (see Table 3), which reveals that the FRESH icebergs lead to an 11.6% greater sea-ice area than DUMMY. This is about twice as much as the 6.2% sea-ice facilitation effect in the experiment with COOL icebergs, which is reflected in the FRESH/COOL ratio given in the far right column of Table 3. The net distribution effect (ICB–CTRL) on the sea-ice area is small (−1.4%) but significant.

The relatively strong impact of the freshening effect on the surface ocean (e.g. twice as large an increase in sea-ice area compared to the cooling effect) is related to its stratifying influence on the water column. The FRESH icebergs dilute the surface ocean by 0.05 psu. Fresher surface waters are more easily frozen, resulting in more wind shielding and heat insulation, and lighter. The result is a more stratified water column, which acts as a positive feedback since less sensible heat is being entrained.

Furthermore, the freshening would affect the strength of the pycnocline as well as the ratio between the heat and salt differences in the pycnocline, both of which can affect the stability of the water column (Martinson, 1990b). The increased stratification results in a 9.1% net reduction in AABW formation relative to DUMMY.

The impact of the COOL icebergs, on the other hand, is less straightforward. The latent heat flux results also in more sea-ice than in DUMMY (+6.2% in sea-ice area, Table 3), either through directly cooling the surface ocean or by compensating for entrained heat. However, combined with the extra brine rejection this cooling destabilizes the water column by increasing the density of the surface waters. This leads to a 4.5% net increase in AABW production compared to DUMMY (Table 3). When the icebergs are both fresh and cool (ICB) the effects more or less add up (Table 3: FRESH and COOL combined).

Interestingly the COOL icebergs lead to a net freshening of the surface ocean, despite the stronger mixing with warmer and saltier intermediate waters. This freshening mostly takes place where the sea-ice anomaly is largest and peaks in summer (Fig. 5). Apparently the increased sea-ice cover not only reduces evaporation (through limiting the area that interacts with the atmosphere) but also acts as a large fresh water buffer that is not released until it melts, along with the snow that fell on top of the ice. This net freshening provides a negative feedback on the destabilizing effect of the cooling latent heat and a positive feedback on sea-ice formation.

So it is clear that in our results sea-ice facilitation and ocean stratification are the dominant feedback mechanisms, which are triggered to a smaller or greater extent by the fresh water and latent heat fluxes from icebergs. From this point of view we can understand the distribution effect, which is spatially complex (Figs. 3E). The discussed feedbacks can be expected to be strongest near the edge of the sea-ice, where slight shifts in surface temperature and/or salinity (that can be caused by the melting icebergs) can significantly affect the sea-ice fraction (Figs. 3-III). Compared to the homogeneous fluxes (ICB–CTL), the dynamic icebergs lead to a 0.08 °C higher SST and 0.015 psu saltier SSS, accompanied by a ∼10% stronger deep water production. However, as shown in Fig. 3, the impact of including dynamic icebergs is spatially highly variable, and results locally in deeper mixing than the classical homogeneous fluxes. One might say that at key locations of deep water formation in the model (in particular in the Eastern Weddell Sea) the dynamically distributed icebergs, which tend to either stick near the coast or take off towards the North–East from the Antarctic Peninsula, are 'less efficient' at stratifying the ocean than the homogeneous fluxes. The net result is slightly (1.4%) less sea-ice area, and 9.7% stronger open ocean convection.

3.4. Discussion of limitations and future outlook

The air/sea/ice system is highly coupled and interactive, and is sensitive to the strength and character of the pycnocline

Table 3
Overview of the results of the sensitivity experiments. Averaged freshening, cooling, combined (FRESH and COOL) and distribution effects on: SSS and SST (south of 50°S); sea-ice area in the Southern Hemisphere and AABW production (yearly maximum of the overturning stream function in the Southern Ocean). Each value represents 13-member ensemble averages over the second 50 yearly averages of each member. With variances (SD^2) calculated as a sum of squared differences of the resulting 650 data points compared to their grand mean, all of the differences presented in this table are significant (*z*-test; $P < 5\%$). As a reference, on the left the values and their standard deviation (SD) are provided for the ICB experiment. See also Fig. 3 and Table 2.

Southern Ocean avg.	Reference value (SD)	Freshening effect (%)	Cooling effect (%)	FRESH and COOL combined (%)	Distribution effect (%)	FRESH/COOL ratio (%)
SSS (psu)	34.240 (0.01)	**−0.055**	**−0.017**	**−0.061**	**0.015**	3.1
SST (°C)	2.04 (0.08)	**−0.38**	**−0.19**	**−0.54**	**0.08**	2.0
Sea-ice (10^{12} m^2)	12.59 (0.37)	**1.46** (11.6)	**0.78** (6.2)	**1.93** (15.3)	**−0.17** (−1.4)	1.9
AABW Prod. (Sv)	−21.60 (1.60)	**1.96** (−9.1)	**−0.97** (4.5)	**1.13 (−5.2)**	**−2.08** (9.7)	−2.0

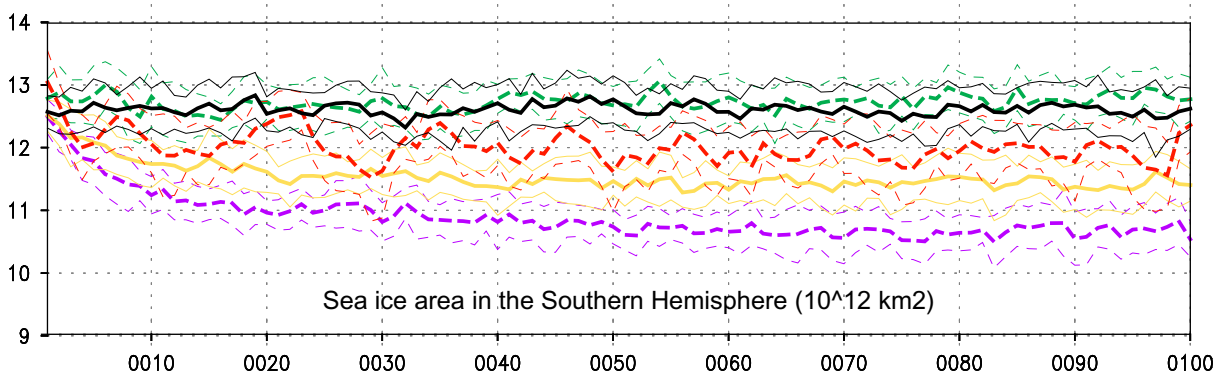

Fig. 4. Time series of averaged sea-ice area (10^{12} m^2) in the Southern Hemisphere for the respective experiments. Top to bottom: green, ICB; black, CTL; red, FRESH; yellow, COOL; purple, DUMMY. The thick lines represent 13-member ensemble means of the yearly averages, while the thin lines mark 1 SD (ensemble standard deviation for that point in time).

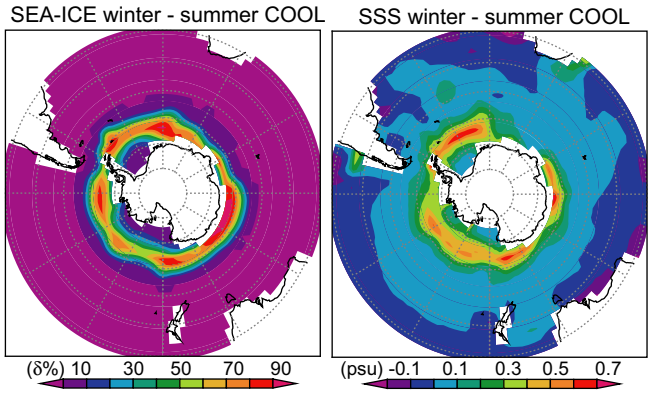

Fig. 5. Sea-ice as a fresh water buffer. Seasonal differences in sea-ice area (left) and sea surface salinity (right) for the icebergs with latent heat flux only (COOL). The reduced salinity pattern in summer (January, February and March) mimics the sea-ice expansion in winter (July, August and September), which apparently acts as a fresh water buffer. Thus sea-ice facilitation by COOL icebergs can lead to reduced surface salinity. Based on monthly averages over the second 50 years of 13 ensemble members.

(Martinson, 1990a,b). According to our results, a more plausible distribution of iceberg-related fluxes can have a significant impact on local convection layer depth as well as overall overturning in the Southern Ocean. It should be noted that the simulated 1–2 Sv change in the AABW production due to the icebergs (Table 3) is smaller than the available estimates for the uncertainty of AABW production (e.g. (Garabato et al., 2002)). However, from a sensitivity-study perspective, what matters is that the anomalies presented are statistically significant within the experimental framework.

However, our results should be confirmed by independent modelling studies, as our coupled model has its limitations. Generally speaking, ECBilt-CLIO overestimates the importance of open ocean convection (Goosse and Fichefet, 2001). Presumably, in the real world shelf convection is more important, involving strong brine rejection associated with continuous sea-ice production in coastal polynyas, which are not captured in our model. Furthermore the grid-size of our ocean is of the same order of magnitude as the critical size of open ocean polynyas. This might affect the persistence of these features, although it has been shown that the model performs reasonably well regarding the location and behaviour of the polynyas (Fichefet and Goosse, 1999; Goosse and Fichefet, 2001).

The iceberg model includes also some simplification (e.g. icebergs are box-shaped and get 'glued' when stranding until their keel is shallower than local grid depth) and so does the coupling (feedback to the atmosphere is neglected; all fluxes are piped to the surface layer of the ocean). One might want to further develop these aspects of the model when studying local (e.g. Pycnocline penetrating) effects or when large amounts of icebergs are involved (e.g. Iceberg armada's in glacial times (Bond et al., 1992; Bond et al., 1999)). An alternative approach could be to simulate the iceberg distribution in a more statistical manner (Clarke and La Prairie, 2001).

We have highlighted differences in effects between a classical homogeneous distribution of fresh water and latent heat fluxes and their spatio-temporal redistribution by dynamic thermodynamic icebergs. It is important to note that we focused on multi-decadal to century scale surface effects in the Southern Ocean, using ensemble-experiments with a duration of 100 years. We note that deep and bottom ocean processes might well take centuries to react and adapt to the kinds of changes we imposed. Both the salt and heat exchanges are crucial for the properties, production and export of Antarctic Bottom water (Goosse and Fichefet, 1999), which in turn can affect North Atlantic deep water formation in a see–saw mechanism (Stocker et al., 1992; Seidov et al., 2001; Stouffer et al., 2007).

4. Concluding remarks

We have studied the role of icebergs in our climate system by performing experiments with the global, coupled atmosphere–ocean model ECBilt-CLIO that includes an interactive iceberg module. The results were compared with results obtained with a version in which "classical" parameterized iceberg fluxes were distributed homogeneously south of 55°S. We focused on the multi-decadal response of the surface climate in the Southern Ocean. The comparison reveals that the heat and fresh water fluxes from the dynamic icebergs are found to be concentrated closer to shore compared to the traditional parameterized flux distribution, except for a greater extent near the Australian continent and a plume of icebergs floating North–East from the tip of the Antarctic Peninsula. As expected, the redistribution of the fluxes by dynamic icebergs leads to spatially variable responses in the Southern Ocean. On the one hand, the dynamical icebergs facilitate sea-ice formation in the Indian and Pacific sector of the Southern Ocean, whereas in key deep water formation sites in the Eastern Weddell Sea, the sea-ice fraction is larger under homogeneous flux conditions. Both heat-entrainment and wind-driven ice-divergence play an important role in such areas (Fichefet and Goosse, 1999; Goosse and Fichefet, 2001), and susceptibility to the wind is a fundamental difference between the dynamical interactive icebergs and the

parameterized fluxes. Overall the dynamical icebergs lead to a 10% greater net AABW production relative to homogeneous fluxes.

To quantify separately the two main effects of dynamical icebergs, i.e. freshening and cooling, we performed additional sensitivity experiments in which one of the two effects was switched off. These sensitivity experiments are compared to a simulation with dummy icebergs (i.e. with both effects switched off). The comparison indicates that both the freshening and cooling effects lead to a significant increase in sea-ice area in the Southern Ocean of 12% and 6%, respectively. The consequences are most pronounced along the sea-ice margin, where this sea-ice facilitation leads to increased surface albedo, as well as enhanced ocean stratification by wind shielding and heat insulation, which further amplify the cooling and freshening of the surface waters. However, the net impacts on deep convection are different for the freshening and cooling by icebergs. The net effect of freshening is reduced AABW formation as the enhanced stratification dominates, whilst the cooling by icebergs results in an overall increase in AABW formation.

Including dynamical icebergs in global coupled climate models can be important because of the sensitive nature of the Southern Ocean stratification. Dynamical icebergs give a more plausible spatiotemporal flux distribution than ad hoc parameterized fluxes (Death et al., 2006). We show that both the fresh water and the latent heat fluxes from dynamic icebergs can have a significant impact on sea-ice formation and the interconnected stability of the surface ocean. Our results illustrate that these local effects of icebergs can affect the overall net deep water production. The significance of these differences can be expected to increase with the amount of icebergs involved, for example for the paleoclimate under "iceberg armada" conditions.

Acknowledgements

We thank J.M. Campin for his contribution to the early development stages of the iceberg model, and G.R. Bigg for sharing implementation details of their iceberg model. J.I.J. and H.R. are supported by the Netherlands Organization for Scientific Research (NWO). H.G. is Research Associate with the Fonds National de la Recherche Scientifique (FNRS-Belgium). This work is supported by the Belgian Federal Science Policy Office, Research Program on Science for a Sustainable Development. All this support is gratefully acknowledged.

References

Beckmann, A., Goosse, H., 2003. A parameterization of ice shelf–ocean interactions for climate models. Ocean Modelling 5 (2), 157–170.

Bigg, G.R., Wadley, M.R., et al., 1996. Prediction of iceberg trajectories for the North Atlantic and Arctic Oceans. Geophysical Research Letters 23 (24), 3587–3590.

Bigg, G.R., Wadley, M.R., et al., 1997. Modelling the dynamics and thermodynamics of icebergs. Cold Regions Science and Technology 26 (2), 113–135.

Bigg, G.R., Wadley, M.R., et al., 1998. Simulations of two last glacial maximum ocean states. Paleoceanography 13 (4), 340–351.

Bond, G., Heinrich, H., et al., 1992. Evidence for massive discharges of icebergs into the North-Atlantic Ocean during the last glacial period. Nature 360 (6401), 245–249.

Bond, G., Kromer, B., et al., 2001. Persistent solar influence on north Atlantic climate during the Holocene. Science 294 (5549), 2130–2136.

Bond, G., Showers, W. et al., 1999. The North Atlantic's 1–2 kyr climate rhythm: relation to Heinrich events, Dansgaard/Oeschger cycles and the little ice age. Mechanisms of global climate change at millennial time scales, American Geophysical Union-deep sea cores-deep sea cores-deep sea cores, 35–58.

Campin, J.M., Goosse, H., 1999. Parameterization of density-driven downsloping flow for a coarse-resolution ocean model in *z*-coordinate. Tellus Series A Dynamic Meteorology and Oceanography 51 (3), 412–430.

Clarke, G.K.C., La Prairie, D.I., 2001. Modelling iceberg drift and ice-rafted sedimentation. In: Straughan, B., Greve, R., Ehrentraut, H., Wang, Y. (Eds.), Continuum Mechanics and Applications in Geophysics and the Environment. Springer-Verlag, Berlin.

Claussen, M., Mysak, L.A., et al., 2002. Earth system models of intermediate complexity: closing the gap in the spectrum of climate system models. Climate Dynamics 18 (7), 579–586.

Covey, C., Taylor, K.E., et al., 1991. Upper limit for sea ice Albedo feedback contribution to global warming. Journal of Geophysical Research-Atmospheres 96 (D5), 9169–9174.

Death, R., Siegert, M.J., et al., 2006. Modelling iceberg trajectories, sedimentation rates and meltwater input to the ocean from the Eurasian Ice Sheet at the Last Glacial Maximum. Palaeogeography Palaeoclimatology Palaeoecology 236 (1–2), 135–150.

Deleersnijder, E., Campin, J.M., 1995. On the Computation of the Barotropic Mode of a Free-Surface World Ocean Model. Annales Geophysicae Atmospheres Hydrospheres and Space Sciences 13 (6), 675–688.

Dowdeswell, J.A., Whittington, R.J., et al., 1992. The sizes, frequencies, and freeboards of east greenland icebergs observed using ship radar and sextant. Journal of Geophysical Research Oceans 97 (C3), 3515–3528.

Driesschaert, E., 2001. Modélisation de la dérive des icebergs en vue d'applications climatiques, mémoire de fin d'études. Institut d'Astronomie et de Géophysique Georges Lemaître. Louvain-la-Neuve, Université Catholique de Louvain, 76.

Eltahan, M., Eltahan, H., et al., 1983. Forecast of Iceberg Ensemble Drift. Offshore 43 (4), 94.

Fichefet, T., Goosse, H., 1999. A numerical investigation of the spring Ross Sea polynya. Geophysical Research Letters 26 (8), 1015–1018.

Garabato, A.C.N., McDonagh, E.L., et al., 2002. On the export of Antarctic Bottom Water from the Weddell Sea. Deep-Sea Research Part Ii-Topical Studies in Oceanography 49 (21), 4715–4742.

Gladstone, R.M., Bigg, G.R., et al., 2001. Iceberg trajectory modeling and meltwater injection in the Southern Ocean. Journal of Geophysical Research Oceans 106 (C9), 19903–19915.

Goosse, H., Fichefet, T., 1999. Importance of ice-ocean interactions for the global ocean circulation: a model study. Journal of Geophysical Research Oceans 104 (C10), 23337–23355.

Goosse, H., Fichefet, T., 2001. Open-ocean convection and polynya formation in a large-scale ice–ocean model. Tellus Series A Dynamic Meteorology and Oceanography 53 (1), 94–111.

Gordon, A.L., 1991. Two stable modes of Southern Ocean winter stratification. In: Chu, P.C., Gascard, J.C. (Eds.), Deep convection and deep water formation in the oceans, vol. 57. Elsevier, Amsterdam, pp. 17–35.

Heinrich, H., 1988. Origin and consequences of cyclic ice rafting in the northeast Atlantic-Ocean during the past 130,000 years. Quaternary Research 29 (2), 142–152.

Jongma, J.I., Prange, M., et al., 2007. Amplification of Holocene multicentennial climate forcing by mode transitions in North Atlantic overturning circulation. Geophysical Research Letters 34 (15).

Loset, S., 1993. Thermal-Energy Conservation in Icebergs and Tracking by Temperature. Journal of Geophysical Research Oceans 98 (C6), 10001–10012.

Manabe, S., Spelman, M.J., et al., 1992. Transient Responses of a Coupled Ocean Atmosphere Model to Gradual Changes of Atmospheric Co_2. 2. Seasonal Response. Journal of Climate 5 (2), 105–126.

Martinson, D.G., 1990a. Evolution of the Southern-Ocean winter mixed layer and sea ice – open ocean deep-water formation and ventilation. Journal of Geophysical Research Oceans 95 (C7), 11641–11654.

Martinson, D.G., 1990b. Southern-Ocean Sea-Ice Interaction - Implications for Climate and Modeling. Transactions of the Royal Society of Edinburgh Earth Sciences 81, 397–405.

Mellor, G.L., Yamada, T., 1982. Development of a turbulence closure-model for geophysical fluid problems. Reviews of Geophysics 20 (4), 851–875.

Opsteegh, J.D., Haarsma, R.J., et al., 1998. ECBILT: a dynamic alternative to mixed boundary conditions in ocean models. Tellus Series A Dynamic Meteorology and Oceanography 50 (3), 348–367.

Petoukhov, V., Claussen, M., et al., 2005. EMIC Intercomparison Project (EMIP-CO_2): comparative analysis of EMIC simulations of climate, and of equilibrium and transient responses to atmospheric CO_2 doubling. Climate Dynamics 25 (4), 363–385.

Rahmstorf, S., Crucifix, M., et al., 2005. Thermohaline circulation hysteresis: a model intercomparison. Geophysical Research Letters 32 (23).

Robe, R.Q. (Ed.), 1980. Iceberg Drift and Deterioration. Dynamics of Snow and Ice Masses. Academic Press, New York.

Seidov, D., Barron, E., et al., 2001. Meltwater and the global ocean conveyor: northern versus southern connections. Global and Planetary Change 30 (3–4), 257–270.

Smith, S.D., 1993. Hindcasting iceberg drift using current profiles and winds. Cold Regions Science and Technology 22 (1), 33–45.

Smith, S.D., Banke, E.G., 1983. The influence of winds, currents and towing forces on the drift of icebergs. Cold Regions Science and Technology 6 (3), 241–'255.

Stocker, T.F., Wright, D.G., et al., 1992. The influence of high-latitude surface forcing on the global thermocline circulation. Paleoceanography 7 (5), 529–541.

Stouffer, R.J., Seidov, D., et al., 2007. Climate response to external sources of freshwater: North Atlantic versus the Southern Ocean. Journal of Climate 20 (3), 436–448.

Stouffer, R.J., Yin, J., et al., 2006. Investigating the causes of the response of the thermohaline circulation to past and future climate changes. Journal of Climate 19 (8), 1365–1387.

Wadhams, P., 1988. Winter observations of iceberg frequencies and sizes in the South Atlantic Ocean. Journal of Geophysical Research 93, 3583–3590.

Wadhams, P., 2007. Icebergs. Encyclopedia of the Antarctic. In: Riffenburg, B. (Ed.), vol. 1. Routledge, New York, pp. 520–526.

Watkins, S.J., Maher, B.A., et al., 2007. Ocean circulation at the Last Glacial Maximum: a combined modeling and magnetic proxy-based study. Paleoceanography 22 (2).
Weeks, W.F., Campbell, W.J., 1973. Towing icebergs to irrigate Arid Lands – manna or madness. Science and Public Affairs Bulletin of the Atomic Scientists 29 (5), 35–39.
Weeks, W.F., Mellor, M., 1978. Some Elements of Iceberg Technology (ADA053431), Cold Regions Research and Engineering Lab Hanover NH, 38.
Zotikov, I.A., Ivanov, Y.A., et al., 1974. Antarctic continental ice discharge, and formation of Antarctic bottom waters. Oceanology Ussr 14 (4), 485–490.